Theory and Applications of Mathematics & Computer Science

(ISSN 2067-2764)
http://www.uav.ro/applications/se/journal/index.php/tamcs

Theory and Applications of Mathematics & Computer Science 3 (1) (2013) 38–55

The Scale-Curvature Connection and its Application to Texture Segmentation

Eli Appleboim[a], Yedidya Hyams[a], Shai Krakovski[a], Chen Sagiv[b], Emil Saucan[c,*]

[a]*Department of Electrical Engineering, Technion, Haifa 32000, Israel*
[b]*SagivTech Ltd., Eliezer Yaffe 37/18, Ra'anana 43451, Israel*
[c]*Department of Mathematics, Technion, Haifa 32000, and Department of Mathematics and Computer Science, The Open University of Israel, Ra'anana 43537, Israel*

Abstract

In this work we establish a theoretical relation between the notions of scale and a discrete Finsler-Haantjes curvature. Based on this connection we demonstrate the applicability of the interpretation of scale in terms of curvature, to signal processing in the context of analysis and segmentation of textures in images. The outcome of this procedure is a novel scheme for texture segmentation that is based on scaled metric curvature. The presented method proves itself to be efficient even when the multiscale analysis is done up to scales of 19 and more. Our main conclusions are that the discrete curvature calculated on sampled images can give us an indication on the local scale within the image, and therefore can be used for many additional tasks in image analysis.

Keywords: Wavelets, scale-space, Finsler-Haantjes curvature, texture segmentation.
2010 MSC: 42C40, 68U10, 51K10.

1. Introduction

Several tasks in image and signal processing require the calculation and usage of scale. Determining the typical scale at some image location can be useful for de-convolution, detection and recognition tasks. The popular image registration algorithms, SIFT (Lowe, 1999) and SURF (Bay *et al.*, 2006) account for the scale at image locations as a pre-processing step for calculating scale invariant key points, that are used in turn for matching.

Typical approaches to calculate scale in the signal processing community rely on analyzing a multi scale representation of the images, via the scale space approach or the wavelet transform.

*Corresponding author
Email addresses: eliap@ee.technion.ac.il (Eli Appleboim), gwavelet gwavelet@gmail.com (Yedidya Hyams), gwavelet gwavelet@gmail.com (Shai Krakovski), chen@sagivtech.com (Chen Sagiv), semil@tx.technion.ac.il (Emil Saucan)

The versatility and adaptability of scale space theory and wavelets for a variety of tasks in Image Processing and related fields is too well established in the scientific community, and the bibliography pertaining to it is far too extensive, to even begin to review it here.

On the other hand, the concept of curvature is well established in the field of computational geometry. Intuitively, scale and curvature are related. High curvature account for phenomenon that happen at smaller scales than those that are related to low curvature. This relation is further stressed analytically and formally in the smooth category, as the curvature of a smooth curve at some point is defined to be the inverse of the squared radius of the osculatory circle at that point so specifically making curvature a function of scale. Curvature decreases as the inverse of the square root of scale (Petersen, 1998).

The multiresolution property of wavelets has been already applied in determining the curvature of planar curves (Antoine & Jaques, 2003) and to the intelligence and reconstruction of meshed surfaces (see, e.g. (Lounsbery *et al.*, 1997), (Valette & Prost, 2004), amongst many others). Moreover, the intimate relation between scale and differentiability in natural images has also been stressed (Florack *et al.*, 1992).

An intriguing issue is whether one can replace the intuitive trade-off between scale and curvature, by a formal concept of *wavelet curvature*, in particular in cases such as the Strömberg wavelets (Strömberg, 1983) that are based on piecewise-linear functions, and if so then,to what extent this can be further extended to the more difficult case of Haar wavelets that are not even piecewise linear and to what extent this can be made general.

Apparently, this can be done by using *metric curvatures* (Blumenthal & Menger, 1970) (and (Saucan, 2006) for a short presentation). It turns out that the best candidate, for the desired metric curvature is the *Finsler-Haantjes curvature*, due to its adaptability to both continuous and discrete settings (see, e.g. (Saucan & Appleboim, 2005), (Saucan & Appleboim, 2009)).

We have first introduced a formal relation between discrete curvature and scale in (Saucan *et al.*, 2010). In the present paper, that represents a continuation of our previous, above mentioned article, we suggest that a simple curvature calculation can replace the tedious work of convolving images with a large number of multi scaled filters. We show how scale and curvature are related to each other, for a variety of families of wavelets. Afterwards we present the Finsler-Haantjes curvature measure for images and develop a novel scheme for texture separation. Our main goal is, however, more far-reaching, namely to try and bridge, at least partly, the the gap between the two basic, largely non-intersecting, approaches prevalent in Image Processing and related fields: The geometric one, that is closely related to the Graphics community philosophy; and the more classical, Fourier Analysis/Wavelets driven one.

The paper is organized as follows: First, we introduce the mathematical background needed and discuss the notion of scale in Section 2.1. We then elaborate on the Finsler-Haantjes curvature in Section 2.2 and introduce the Fisler-Haantjes curvature of wavelets and for images in Section 3. In section 4 we suggest a scheme for texture analysis in images that is based on our discrete scaled curvature measure. In addition to texture segmentation there is a huge variety of further possible applications to the ideas and methods presented herein, as well as open issues for further research. Some of those are mentioned in Section 5 in which we summarize the paper.

2. Mathematical Background

In this section we present both the notion of scale and that of the Finsler-Haantjes Curvature. While these two components are derived from completely different worlds, we show that they are strongly related to each other.

2.1. The Notion of Scale

The notion of scale is fundamental in many mathematical and applicative discussions. Scale is one of these terms that has a clear intuitive meaning, but is hard to be defined mathematically. The question of finding a measure for calculating the local scale in signals and images has been addressed in the past in the context of scale space analysis and wavelets transform. It plays a significant role in the framework of image matching and registration, where scale invariant descriptors are desired. Evaluating the dominant scale within image data is highly important for real life applications. For a computer vision system analyzing an unknown scene, there is no way to know a priori what scales are appropriate for describing the interesting structures in the image data. Hence, the only reasonable approach is to consider descriptions at multiple scales in order to be able to capture the unknown scale variations that may occur. Scale-space theory is a formal theory for handling image structures at different scales, by representing an image as a one-parameter family of smoothed images, the scale-space representation. This representation is parameterized by the size of the smoothing kernel used for suppressing fine-scale structures.

In the early eighties Witkin (Witkin, 1983a),(Witkin, 1983b) proposed to consider scale as a continuous parameter and formulated the principal rules of modern scale-space theory relating image structures represented at different scales. Since then, scale-space representation and its properties have been extensively studied and important contributions have been made by Koenderink (Koenderink, 1984), Lindeberg (Lindeberg, 1998) and Florack (Florack *et al.*, 1992). In many cases it is necessary to select locally appropriate scales for further analysis. This need for scale selection originates from the need to process real-world objects that may have different sizes and because the distance between the object and the camera can vary. The seminal work of Lindenberg (Lindeberg, 1998) dealt with the issue of automatic scale selection. The idea was to determine the characteristic scale for which a given function attains an extremum over scales. The name characteristic is somewhat arbitrary as a local structure can exist at a range of scales and within this range there is no preferred scale of perception. However, a scale can be named characteristic, if it conveys more information comparing to other scales. In his work, Lindenberg noted that a highly useful property of scale-space representation is that image representations can be made invariant to scales, by performing automatic local scale selection based on local maxima (or minima) over scales of normalized derivatives.

This work served as the basis for tasks such as blob detection, corner detection, ridge detection and edge detection. Scale space theory is fundamental for detecting invariant features within signals and images that can be used for various tasks such as registration, detection and recognition among others. Multi-scale representation of data is crucial for extracting local features used for determining regions of interest for subsequent detection of scale-invariant interest points for computing image descriptors, most notable are the SIFT (Lowe, 1999) and SURF (Bay *et al.*, 2006) frameworks.

Both the SIFT and the SURF algorithms rely on Scale-space extrema detection, where the first stage of computation searches over all scales and image locations. It is implemented by using a Laplacian-of-Gaussian or a difference-of-Gaussian function to identify potential interest points that are invariant to scale and orientation.

A common practice for scale determination relies on the convolution of the data with a bank of functions that have different scales. The characteristic scale usually corresponds to the local extremum of the convolution results, taken over scales. The characteristic scale is related to structure. The common methodology for finding this exterma values in scale space involves analysis of the behavior of the Laplacian of Gaussian (Bay *et al.*, 2006), Difference of Gaussian (Lowe, 1999) and the Hessian matrix to name a few. There are strong relations between scale-space theory and wavelet theory, although these two notions of multi-scale representation have been developed from somewhat different premises. Wavelets are multi scaled versions of a specific mother function, thus when convolving them with data, one can exploit the scale contents of that data, in a very similar way that the frequency contents of data can be expressed using the Fourier transform. A strong response to a wavelet function with a certain support and scale, suggests that there is significant information at that scale at that image location.

2.2. The Finsler-Haantjes Curvature

The most intuitive definition for curvature is the amount by which a geometric object deviates from being flat, or straight in the case of a line. It is natural to define the curvature of a straight line to be identically zero. The curvature of a circle of radius R should be large if R is small and small if R is large. Thus the curvature of a circle is defined to be the reciprocal of the squared radius (do Carmo, 1976).

The following metric definition for curvature is due to Haantjes, following an idea of Finsler (Blumenthal & Menger, 1970):

Definition 2.1. *Let (M,d) be a metric space, let* $c : I = [0,1] \tilde{\to} M$ *be a homeomorphism, and let* $p, q, r \in c(I),\ q, r \neq p$. *Denote by* $\widehat{qr}$ *the arc of* $c(I)$ *between* q *and* r, *and by* qr *the segment from* q *to* r. *We say that* c *has* Finsler-Haantjes curvature $\kappa_{FH}(p)$ *at the point* p *iff:*

$$\kappa_{FH}^2(p) = 24 \lim_{q,r \to p} \frac{l(\widehat{qr}) - d(q,r)}{(d(q,r))^3}\ ; \tag{2.1}$$

where "$l(\widehat{qr})$*" denotes the length, in intrinsic metric induced by* d, *of* $\widehat{qr}$ *– see Figure 1. (Here we assume the curve* $c(I)$ *is* rectifiable, *hence that, in particular, the arc* $\widehat{qr}$ *has finite length.)*

This definition of curvature represents, indeed, a proper adaptation, for an extensive class of curves in quite general metric spaces, of the classical notion of curvature, as proven by the following

Theorem 2.1. *Let* $c \in C^3(I)$ *be a smooth curve in* $\mathbb{R}^3$, *and let* $p \in c$ *be a regular point. Then* $\kappa_{FH}(p)$ *exists and, moreover,* $\kappa_{FH}(p) = k(p)$ *– the classical (differential) curvature of* c *at* p.

Remark. Originally the Finsler-Haantjes curvature is defined with $l(\widehat{qr})$ appearing in the denominator instead of $d(q,r)$, ((Blumenthal & Menger, 1970)). We have opted for the above definition

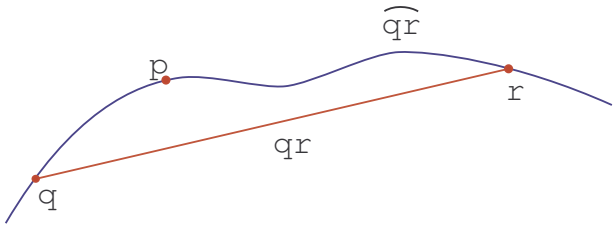

Figure 1. A (metric) arc and its corresponding chord (metric segment).

for practicality reasons. Moreover, in the setting of this work (and, in fact, in a much more general context) the above theorem still holds with our modified definition, therefore the definition used herein is interchangeable with the original one (see, again (Blumenthal & Menger, 1970)).

3. Finsler-Haantjes Curvature for Wavelets and Images

In this section we consider a semi-discrete (or semi-continuous) version of the Finsler-Haantjes curvature, and then introduce this curvature measure in the case of a wavelet function.

3.1. Semi-discrete Finsler-Haantjes Curvature

Consider a typical piecewise-linear wavelet φ, such as the one depicted in Figure 2, let $\widehat{AE}$ be the arc of curve between the points A and E, and let $d(A, E)$ is the length of the line-segment AE.

Then

$$l(\widehat{AE}) = a + b + c + d \ \ ; d(A, E) = e + f. \tag{3.1}$$

The following discretization of formula (2.1) is, therefore, natural:

$$\kappa^2_{FH}(\varphi) = 24[(a + b + c + d) - (e + f)]/(e + f)^3. \tag{3.2}$$

In addition to the total curvature of the wavelet φ, one can also compute the "local" curvatures of the partial wavelets $\varphi_1 = \widehat{ABC}$ and $\varphi_2 = \widehat{CDE}$, that is the curvatures at the "peaks" B and D:

$$\kappa^2_{FH}(B) = 24(a + b - e)/e^3 \ , \tag{3.3}$$

and

$$\kappa^2_{FH}(D) = 24(c + d - f)/f^3 \ , \tag{3.4}$$

as well as the mean curvature of these peaks:

$$H_{FH}(\widehat{AE}) = [\kappa_{FH}(B) + \kappa_{FH}(D)]/2. \tag{3.5}$$

Even though these variations may prove to be useful in certain applications, we believe that the correct approach, in the sense that it best corresponds to the scale of the wavelet, would be to compute the total curvature of φ. However, had the definition of Finsler-Haantjes curvature been limited solely to piecewise-linear wavelets, its applicability would have also been diminished. We show, however, that it is also definable for the "classical" Haar wavelets, in a rather straightforward manner.

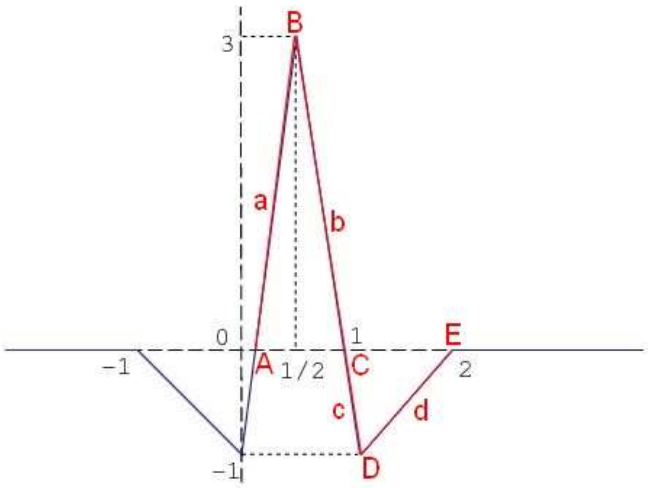

Figure 2. A typical piecewise-linear wavelet (red), part of the Meyer Wavelet (Meyer, 1993) (blue and red).

Remark. In the sequel we will therefore omit the coefficient $\sqrt{24}$ for convenience.

3.2. *Finsler-Haantjes curvature of Haar Wavelets*

For every $s \in \mathbb{Z}$ let $j = 2^s$, and let Ψ_j denote the Haar wavelet at scale j and with zero shift, where $\Psi_1 = \Psi$ is the mother wavelet of Haar basis, considered in the above example. Then Ψ_j can be presented as:

$$\Psi_j = \begin{cases} j^{-1}, & x \in (0, \frac{j}{2}); \\ -j^{-1}, & x \in (\frac{j}{2}, j); \\ 0 & otherwise. \end{cases} \tag{3.6}$$

Then, in the notations of Figure 2 we have that $A = 0, E = j$, so we have that $l(\widehat{AE}) = 4 \cdot j^{-1} + j$, and $d(\widehat{AE}) = j$, therefore for these wavelets the Finsler-Haantjes curvature satisfies:

$$\kappa^2_{FH}(\Psi_j) = \frac{(4 \cdot j^{-1} + j) - j}{j^3} = 4 \cdot j^{-4} \tag{3.7}$$

The Finsler-Haantjes curvature is certainly invariant under shifts therefore the same dependency of K_{FH} in scale is the same for shifted Haar wavelets as well.

3.3. *Finsler-Haantjes curvature of Walsh Basis*

Let R_s be the Rademacher function which takes the value $1, -1$ on the dyadic intervals $[\frac{j}{2^{s+1}}, \frac{j+1}{2^{s+1}})$, $j = 0, 1, ..., 2^{s+1}$ of the unit interval. Figure 3 shows the first four Rademacher functions.

Then for any $k \in \mathbb{N}$, if we take the binary expansion of k as a sum of powers of 2, $k = 2^{p_1} + 2^{p_2} + \cdots + 2^{p_m}$, and define the k_{th} Walsh function as ((Beauchamp, 1975)):

$$W_k = R_{p_1} \cdot R_{p_2} \cdots R_{p_m} \tag{3.8}$$

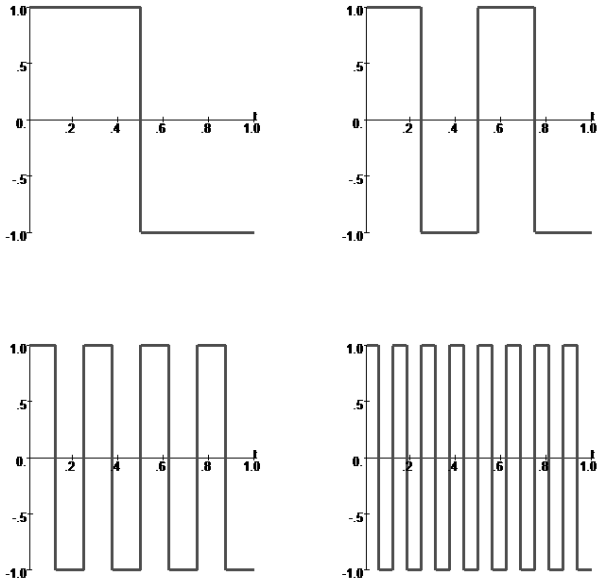

Figure 3. First four Rademacher functions.

Again, in the notations of Figure 2 we have that, $A = 0, E = 1, l(\widehat{AE}) = 2 \cdot 2^s + 1, d(\widehat{AE}) = 1$ which results with

$$\kappa^2_{FH}(W_s) = \frac{(2 \cdot 2^s + 1) - 1}{1^3} = 2^{s+1} \ . \tag{3.9}$$

Although the Walsh basis is not a wavelet basis (see (Beauchamp, 1975)), we can easily regard the function W_s as a function in a specific scale which is $j = \frac{1}{s+1}$ hence the curvature of the Walsh function at scale j is $2^{\frac{1}{j}}$.

For a smooth wavelet Ψ, compactly supported, we can of course define its Finsler-Haantjes, K_{FH} by taking $l(\widehat{AE})$ to be the usual arc length given by $\int_{\text{support}\Psi} \sqrt{1 + \Psi'^2}$.

3.4. Curvature vs. Scale

By an analysis similar to those in Sections 3.2 and 3.3, we will be able to compute a specific dependency of the Finsler-Haantjes curvature as a function of scale, for every family of piecewise constant wavelets. Moreover, with only a limited amount of additional effort, this goal is also achievable for the families of piecewise linear wavelets. This correlation most probably depends on the specific family under consideration. Indeed, as already noted above, Haar wavelets behave differently from the Walsh basis as far as the curvature vs. scale correspondence is concerned. To obtain a similar relation in the case of smooth wavelets, one should recall that if Ψ_j is a smooth wavelet function at some scale j, then it can be approximated, for instance, in the L_2-norm, by a sequence of Haar functions. More precisely, for every $\epsilon > 0$, there exists $k = k(j, \epsilon) \in \mathbb{N}$, such that

$$\int_{\text{supp}\Psi_j} |\Psi_j - \sum_i^k Haar_i|^2 < \epsilon \ . \tag{3.10}$$

Combining the inequality above with Equation (3.7) we obtain that the Finsler-Haantjes curvature of Ψ will display a scale-curvature relation similar with that observed for the Haar wavelet. Here, by "similar" we mean that it will decrease as curvature increases. However, we probably cannot expect in this case a simple analytic expression comparable with the one displayed in the case of Haar wavelets. The precise behavior, if can be derived at all, is left as an open question at this point. It would be reasonable to assume that it depends on the specific wavelet family Ψ, as well as on the proximity factor ϵ. Nevertheless, this behavior is indeed demonstrated in the numerical tests that were applied on a variety of wavelets families. For each type of wavelets, Haantjes curvature was computed for the wavelets families at different scales. The general behavior is similar in all different families and are shown in Figure 4. It is shown that, as expected, curvature decreases as scale increases. As indicated by Equation (3.7), we see that the decrease of curvature as a function of scale for the Haar wavelet is different then the one of classical differential geometry of smooth manifolds, where the decrease has a magnitude of $(scale)^{-2}$, while for the Haar wavelet it was shown to be in a magnitude of $(scale)^{-4}$. The difference evidently follows from the fact that we compute the Finsler-Haantjes curvature in a global way rather than locally, as usually curvature is computed in the classical differential geometric setting.

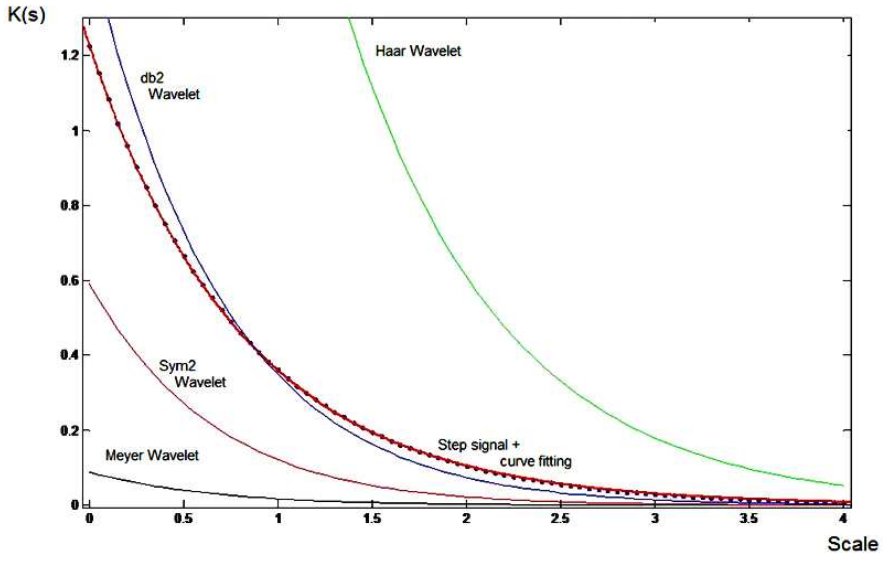

Figure 4. Curvature as a function of scale for a number of standard wavelets: The Haar wavelets, db2 wavelets, sym2 wavelets, the Meyer wavelets; as well as the step signal.

3.5. Curvature for images

From the definition of Finsler-Haatjes for curves we can easily define a discrete version of curvature for surfaces in general, and for images in particular. For say, a point x on a surface Σ, the most natural thing to do is to consider Fisler-Haantjes curvature in any of the directions emanating from x, then find the maximal and minimal curvatures, and then take either the mean of these two

values so to obtain a Finsler-Haantjes *mean curvature* or, alternatively take the multiplication of these two in order to obtain a Finsler-Haantjes version of the *Gaussian curvature* at x. We adopt this concept to images while we consider an image as a surface embedded in some $\mathbb{R}^n$. A gray scale image, for example, can naturally be considered as a surface in $\mathbb{R}^3$. In this case the Finsler-Haantjes curvature is computed at each pixel in four different directions and then the average of these four curvatures is taken. This is done in the framework that was defined in Equation 3.3 of localized curvature, where for images the localization is done by considering a window of some size $n \times n$ centered at the pixel. Each of the images shows the results of computing this version of mean curvature as computed for window sizes of 3×3, 5×5 and 7×7.

Before we proceed further, let us briefly discuss a limit case: If a signal (image) displays a unique scale, e.g. for periodic signals, for which there is a direct correlation between scale and the period T, one expects that to observe that the graph of the curvature function is the smoothest precisely in windows of size T. That this is indeed the case is illustrated in Figure 5.

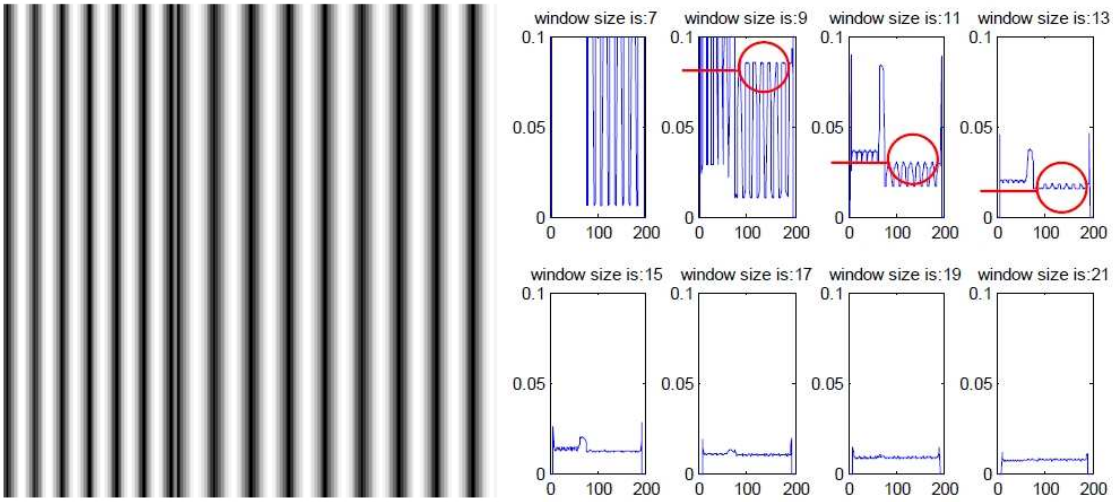

Figure 5. Left: A test image, consisting of two *sin* signals of different periods (11 pixels – left, and 15 pixels – right). Right: As expected, on the windows corresponding to the period of the signal (image) the curvature graph is the most smooth. (Notice the highlighted "windows".)

We clearly can see how Haanjes-Finsler curvature performs as an edge detector. This result is expected, since curvature, even its metric, abstract setting, still has qualities similar to those of a second derivative. This is clearly illustrated in Figure 6. This is further emphasized in the more challenging example in Figure 7, of a satellite image of the Egypt pyramids at Giza, as they lie against the background of sand dunes and opposed to the adjacent neighbourhood of Cairo. It should be noted that, curvature map in itself can serve as a good man made detection tool in arial and satellite images.

Figure 6. Haantjes-Finsler curvature of an image with respect to different scales. From top left in clockwise direction: original image, $3X3$, $7X7$ and $5X5$ window size.

4. Texture segmentation

As a possible application of the proposed method of indicating scale via curvature we look at the problem of image texture segmentation. The novel segmentation scheme yielded from this approach is outlined below.

1. At each pixel Haantjes-Finsler curvatures are computed at different scales and different orientations. For each window, curvatures are computed in 4 directions, horizontal vertical and two diagonal directions $\kappa_h, \kappa_v, \kappa_{d_1}, \kappa_{d_2}$. Finally, the average $\kappa_{Avg} = (\kappa_{Max}(pix) - \kappa_{min}(pix))/\kappa_{Max}(pix)$ of these four obtained curvatures is taken as the curvature at the pixel in the relevant scale. (The specific average considered here was inspired by the standard Image Processing definition of the contrast $C(I)$ of an image I, $C(I) = (I_{Max} - I_{min})/I_{Max}$.) This approximates the average curvature at each scale. The outcome of this step is a vector of length m where m is the number of different scales, $V(pix, scale)$ where pix denotes pixel, and each entry of the vector represents the average curvature at the corresponding scale.

2. Next, at each pixel, the gradient, with respect to scale $\nabla_{scale}V$, of this curvature vector is computed, and we look for the scales at which the gradient exceeds a predefined threshold. (Note that, at this point, curvature and scale are already interchangeable.) Afterwards, all scales which fulfill the threshold criteria are averaged in order to get a scalar value for each pix. The average scale is the outcome of this step. We consider this scale as the scale of important information at the relevant pixel.

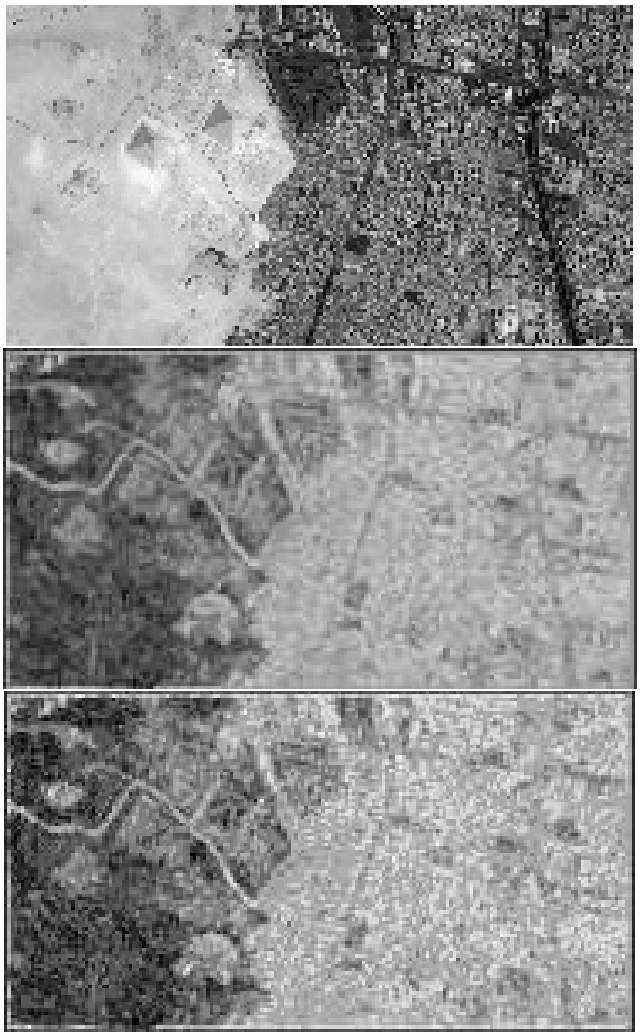

Figure 7. Haantjes-Finsler curvature of a satellite image with respect to different scales. From top to bottom: original image, curvature averaged on 3X3 windows, curvature averaged on 7X7 windows.

3. The output of previous step is a matrix in the same size as the image size, each entry of which is the scale of information at the relevant pixel. A smoothed version of this matrix is obtained by a linear filtering at size which is compatible with the amount of localized information one wishes to obtain. Segmentation to small textures will require small filtering support.

4. We segment the image according to the smoothed information scale computed in the previous step. Pixels with similar scales are grouped together to form different segments. The segmentation is done after curvature values are quantized to several levels. In the experiments shown herein quantization is taken into seven levels.

The procedure detailed above is summarized as Algorithm 1, which is divided into its four main constituent parts:

Input: Grayscale image I
Output: Vector $V(pix, scale)$ of length m = number of scales
foreach *pixel pix in I* **do**
  foreach *window of size* $\leq m$ **do**
    compute $\kappa_h(pix), \kappa_v(pix), \kappa_{d_1}(pix), \kappa_{d_2}(pix)$ and find $\kappa_{Max}(pix), \kappa_{min}(pix)$;
    compute $\kappa(pix) = \kappa_{Avg}(pix) = \frac{\kappa_{Max} - \kappa_{min}}{\kappa_{Max}}$;
  end
end

Input: $V(pix, scale)$
Output: Matrix $M(I)$ – The average scale matrix
foreach *pixel pix in I* **do**
  compute $\nabla_{scale} V$;
  choose scale threshold s_0;
  select scales s_i for which $V(pix, scale) > s_0$;
  compute $s_{Avg} = s_{Avg}(pix) = \frac{\sum s_i}{|\{s_i \,|\, V(pix,scale) > s_0\}|}$;
end

Input: $M(I)$
Output: Matrix $\widetilde{M}(I)$ – Smoothed version of $M(I)$
choose window size $w_0 = w_0(texture)$;
apply linear filter at size w_0;

Input: $\widetilde{M}(I)$
Output: Segmented image $\tilde{I}$
choose maximal number of quantization levels q_0;
foreach *pixel pix in I* **do**
  compute the quantized values $\bar{s}_{Avg}(pix)_j\,,\ j = 1, \ldots, q_0$;
end
group pixels in segments $\mathfrak{s}_l(j) = \{pix \,|\, \bar{s}_{Avg}(pix) = \bar{s}_{Avg}(pix)_j\}$;

Algorithm 1: Segmentation algorithm.

In the following figures, first results of the proposed method are shown for different images. Figure 8 shows the original synthetic image which is comprised of two different textures, the second image in the figure shows the gradient vector $\frac{\partial}{\partial scale} V(scale, pixel)$ of the scaled curvature vector V, while in the third image we see the gradient vector field after smoothing with a filter of size 3×3, and in the fourth image the outcome segmentation is shown after quantization of the smoothed gradient into 4 levels. In the segmented image we see intermediate texture around the internal circle. When one looks at the original image we can clearly see that this is caused by those pixels that are in the intersection of the two different ares of the images and indeed we cannot associate specific texture to these pixels.

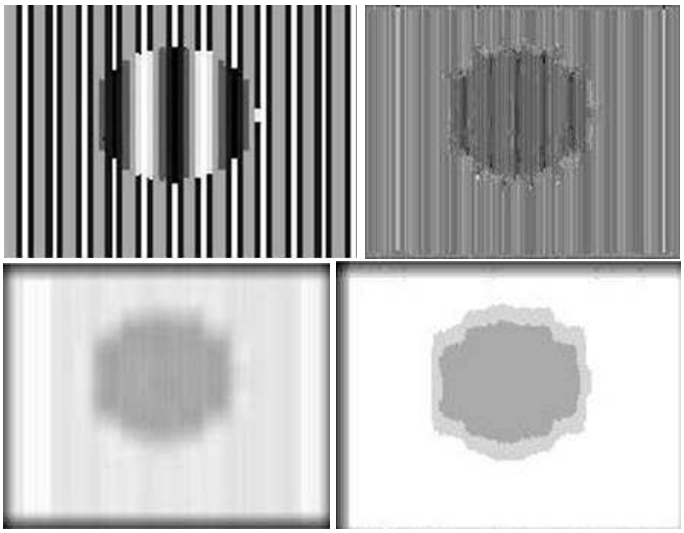

Figure 8. Segmentation of two synthetic textures: From top to bottom and from left to right: Original image, averaged information scales, smoothed gradient of the scaled curvature, the outcome of the segmentation process after quantization into 4 levels.

In Figure 9 from top to bottom we see the original image, averaged information scales as depicted in the second step of the algorithm described above and the outcome of the segmentation process after smoothed by $3X3$ window and quantized to 7 levels. Notice the sensitivity of segmentation to texture.

Figure 9. Segmentation of mandrill image. From left to tight: Original image, averaged information scales, the outcome of the segmentation process after smoothed by $3X3$ window and quantized to 7 levels.

Figure 10 shows similar phenomena on an image of fabric with several textures. The figure shows the original image and the segmented outcome of the process. We can see good separation between the different textures.

The efficiency of the proposed the segmentation algorithm is highlighted on what might be called the ”semi -synthetic” (due to the regularity and quasi-periodicity of this natural image) of

the stairs – see Figure 11.

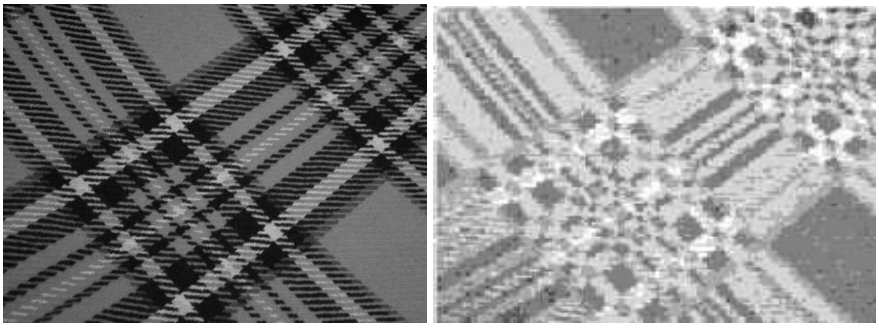

Figure 10. Segmentation of fabric image, window size and quantization level as in Figure 9. Although filter size is small one can easily see good differentiation between different structures along the fabric.

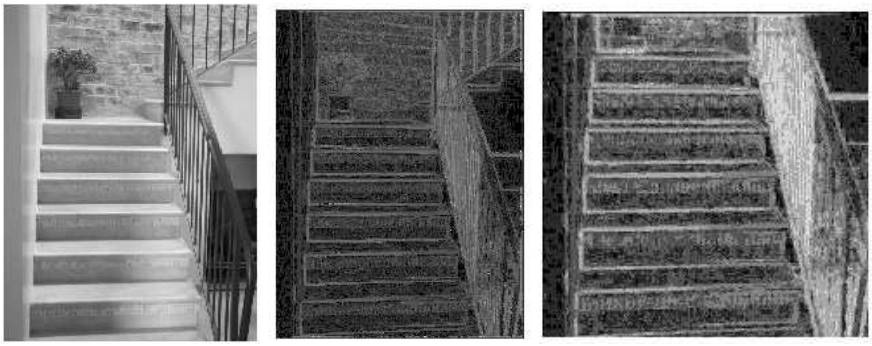

Figure 11. Segmentation of the stairs image: Original image (left), curvature computed using 3*X*3 windows (middle), detail of the segmented image using the same window size (right).

Finally, in Figure 12 the zebras are distinguished from the background of the image after their texture is segmented and separated from the texture of the background.

We conclude this Section with some preliminary comparison results. The briefness of this part is a direct consequence of the main goal of this paper, as stated in the introduction, and which we reiterate here briefly: Our essential objective is to continue and further develop the theoretical framework proposed in (Saucan *et al.*, 2010), that, in our opinion, allows, perhaps for the first time, to integrate, in a unique setting, the two common paradigms of Image Processing, namely the Harmonic Analysis/Wavelets and the Geometric (Graphics related) ones. Therefore, the present endeavor should be viewed rather as a feasibility check, rather that a bourn per se.

Nevertheless, some first comparisons were made, and we gaged our method by likening it with an established method for texture segmentation (Brox & Weickert, 2006) in conjunction with the use of the classical Gabor wavelets. Some of these results are presented in Figure 13.

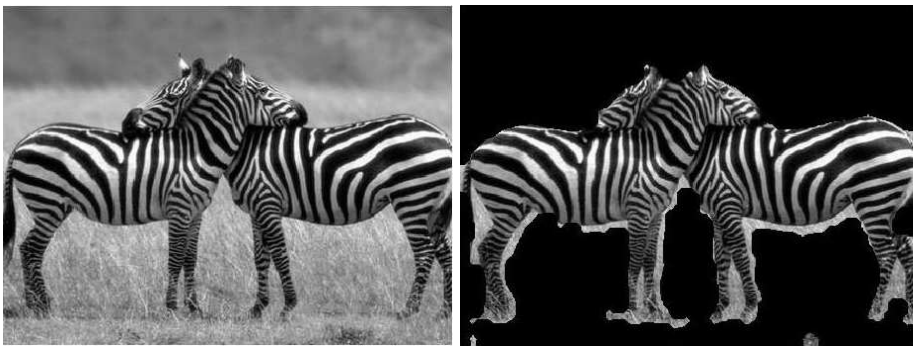

Figure 12. The zebras are extracted from the background of the original image. Extraction is based on the proposed texture segmentation.

5. Summary

The concept of scale is important for several image processing tasks. The calculation of scale on real life data usually relies on the convolution of the data with multi scale filter, where Gaussian derivatives are widespread. In this work we explored the relation between the concept of scale, to curvature. We have used the discrete definition proposed by Haantjes, and have established the theoretical exponential relation that is expected from geometry.

In addition, we propose to use the simpler curvature calculation as a means for automatic scale selection. In that respect, we show two interesting useful applications of the concept of curvature: as edge detectors and for the task of texture segmentation.

As we have noted in the introduction, scale and curvature are simply two manifests of the same physical phenomenon, it should evidently be that scale and curvature calculation can be inter-changed to accomplish the same tasks. However, while for scale only practical, intuitive, but not fully formalized definitions are given even in the most classical textbooks and other such authoritative sources, curvature – even metric one – is a classical, fully established and technical mathematical notion. We propose, therefore, in view of the remark above, to formally define scale by means of the Finsler-Haantjes curvature, at least in the purely theoretical setting. This is more relevant in the context of 2-dimensional (as well, of course, as higher dimensional ones), nonseparable signals, where a proper notion of scale is far less intuitive then in the 1-dimensional, classical, case.

Moreover, we suggest, to use this idea, not only for texture segmentation, but also in many other applications that make use of scale analysis of signals in general and of images in particular. Due to the efficiency of the computation of Haantjes curvature relative to, for instance, wavelets and Gabor functions computations in many scales, we can regard for applications both in image processing, as well as machine vision, where usually efficiency is essential. Just to name a few, we suggest the following,

a Compression and compress sensing.

b Detection of key points in images and registration.

c Scale space representation.

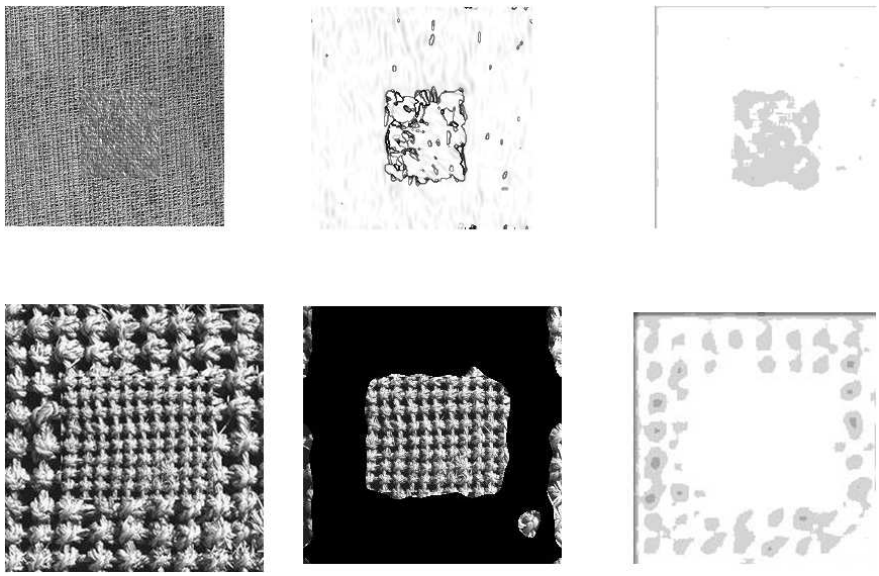

Figure 13. Texture segmentation: Gabor wavelets based segmentation (above) versus curvature based segmentation (below).

d Adaptive edge detection.

e Object recognition.

As for further possible research issues we believe that what we have presented in this paper is actually the tip of an iceberg as far the scale-curvature connection is concerned. Again, to name a few we can mention the following directions,

a Automatic scale selection in the sense of pointing out automatically a scale up to which one can apply analysis-synthesis process with a guaranteed accuracy

b Use additional information which is obtained during the process for additional tasks. As the curvature is computed we gain information about all scales at which, the curvature jumps above a predefined threshold. The method presented herein only makes use of the average of all these scales however one can employ this information for an adaptive scale selection making use of the relevant information of each of these.

c In addition to the above, there is also information about the various directions at which curvature is computed, which is obtained during the process and this information can certainly be exploited for a variety of implementations such as those mentioned above.

d Can we use the curvature-scale relation in order to gain information about the "adequacy" of a certain wavelet family to a given signal? For instance, it is often asked, is it beneficial, in any way, to decompose say, a natural image using a specific wavelets family over the others, say, for obtaining sparse representation? We hope that some answers can be given for this challenging question, via the scale-curvature analysis. We suggest to account for e.g., the exponential decay

of curvature as a function of scale, for the given signal, and then looking for the wavelet family with most similar behavior. In fact this particular question was the one that motivated this line of research.

Acknowledgments

Emil Saucan's research was partly supported by Israel Science Foundation Grants 221/07 and 93/11. and by European Research Council under the European Communitys Seventh Framework Programme (FP7/2007-2013) / ERC grant agreement nº [203134].

References

Antoine, J.P. and L. Jaques (2003). Measuring a curvature radius with directional wavletes. In: *GROUP 24: Physical and Mathematical Aspects of Symmetries, Inst. Phys. Conf. Series*. In J-P. Gazeau, R. Kerner, J-P. Antoine, S. Metens, J-Y. Thibon, (Eds.) **173**(8), 899–904.

Bay, H., T. Tuytelaars and L. Van Gool (2006). SURF: Speeded Up Robust Features. *Lecture Notes in Computer Science* **3951**, 404–417.

Beauchamp, K.G. (1975). *Walsh Functions and Their Applications*. London Academic Press.

Blumenthal, L.M. and K. Menger (1970). *Studies in Geometry*. Freeman & co., San Francisco.

Brox, T. and J. Weickert (2006). A TV flow based local scale estimate and its application to texture discrimination. *Journal of Visual Communication and Image Representation*. **17**(5), 1053–1073.

Cohen, L. (1993). The Scale Representation. *IEEE Trans. Signal Processing*. **41**(12), 3275–3292.

do Carmo, M.P (1976). *Differential Geometry of Curves and Surfaces*. Prentice-Hall, Englewood Cliffs, NJ.

Florack (1997). Image Structure. *Computational Imaging and Vision* **10**. Kluwer Academic Publishers, Dordrecht.

Florack, L., B.M. ter Haar Romeny, J.J. Koenderink and M.A. Viergever (1992). Scale and the differential structure of images. *Image Vision Comput.* **10**(6), 376–388.

Koenderink, J.J. (1984). The structure of images. *Biological Cybernetics*. **50**, 363–370.

Lindeberg, T. (1998). Feature detection with automatic scale selection. *International Journal of Computer Vision*. **30**, 77–116.

Lounsbery, J.M., A.D. DeRose and J. Warren (1997). Multiresolution Analysis For Surfaces Of Arbitrary Topological Type. *ACM Transactions on Graphics*. **16**(1), 34–73.

Lowe, D.G. (1999). Object recognition from local scale-invariant features. *ICCV '99*. **2**, 1150–1157.

Meyer, Y. (1993). *Wavelets : Algorithms & Applications*. SIAM, University of Michigan, MI.

Petersen, P. (1998). *Riemannian Geometry*. Springer-Verlag, New York.

Saucan, E. (2006). Curvature – Smooth, Piecewise-Linear and Metric. In: *What is Geometry?, Advanced Studies in Mathematics and Logic*. G. Sica, (Ed.), pp. 237-268

Saucan, E. and E. Appleboim (2005). Curvature Based Clustering for DNA Microarray Data Analysis. *Lecture Notes in Computer Science* **3523**, 405–412.

Saucan, E. and E. Appleboim (2009). Metric Methods in Surface Triangulation. *Lecture Notes in Computer Science* **5654**, 335–355.

Saucan, E., C. Sagiv and E. Appleboim (2010). Geometric Wavelets for Image Processing: Metric Curvature of Wavelets. In: *Proceedings of SampTA 2009, France, Marseille, May 18-22, 2009*. pp 85–89.

Strömberg, J.O. (1983). A modified Franklin system and high order spline systems on $\mathbb{R}^n$ as unconditional bases for Hardy spaces. In: *Conference on Harmonic Analysis in honor of A. Zygmund*. Wadeworth International Group, Belmont, CA. W. Beckner, (Ed.), pp 475-494.

Valette, S. and R. Prost (2004). Wavelet-Based Multiresolution Analysis Of Irregular Surface Meshes. *IEEE Transaction on Visualization and Computer Graphics*. **10**(2), 113–122.

Witkin, A.P. (1983). Scale-space filtering. In: *Proceedings of the Eighth international joint conference on Artificial intelligence*. Vol. 2, pp. 1019–1022.

Witkin, A.P. (1983). Scale Space Filtering: A New Approach to Multi-Scale Descriptions. In: *Proc. 8th Int. Joint Conf. Art. Intell., Germany, Karlsruhe*. pp. 1019–1022.